Journal for ImmunoTherapy of Cancer

Targeting IL13Rα2 in melanoma with a bispecific T-cell engager: expression profiling and preclinical evaluation

Shushu Zhao ,[1] Yeqing Chen,[1] Pratik S Bhojnagarwala ,[1] Cory Livingston,[1] Joshua Jose ,[1] Yangcheng Gao,[2] Daniel H Park ,[1] Meenhard Herlyn,[1] David B Weiner [1]

To cite: Zhao S, Chen Y, Bhojnagarwala PS, *et al*. Targeting IL13Rα2 in melanoma with a bispecific T-cell engager: expression profiling and preclinical evaluation. *Journal for ImmunoTherapy of Cancer* 2025;**13**:e011073. doi:10.1136/jitc-2024-011073

► Additional supplemental material is published online only. To view, please visit the journal online (https://doi.org/10.1136/jitc-2024-011073).

Accepted 23 May 2025

[1]Wistar Institute of Anatomy and Biology, Philadelphia, Pennsylvania, USA
[2]University of Pennsylvania, Philadelphia, Pennsylvania, USA

Correspondence to
Dr David B Weiner;
dweiner@wistar.org

ABSTRACT

Background Melanoma is a highly aggressive skin cancer, especially in advanced stages. While current treatments such as targeted therapies and immunotherapies have made significant progress, challenges like drug resistance and limited effectiveness in some patients persist. Therefore, ongoing development of novel therapies, particularly for late-stage melanoma, is crucial.

Methods In this study, we explored the expression of interleukin-13 receptor subunit alpha-2 (IL13Rα2) in melanoma patient-derived xenograft models. We investigated IL13Rα2 as a potential target for melanoma treatment by employing an IL13Rα2-CD3 bispecific T-cell engager (BTE). We tested the effect of IL13Rα2-CD3 BTE on T cell activity by flow cytometry. We studied the potency of IL13Rα2-CD3 BTE in tumor killing assay in vitro. For in vivo studies, we administered DNA expression cassettes encoding IL13Rα2-CD3 BTE (IL13Rα2-CD3 DNA encoding BTE (dBTE)) into immunodeficient mice for direct in vivo expression. The mice were challenged with A375 cells and then treated with IL-13Rα2-CD3 dBTE versus control and reconstituted with human peripheral blood mononuclear cells (PBMCs) or T cells. Tumor development was monitored, and T cell infiltration in the tumor was analyzed throughflow cytometry.

Results Our findings revealed heterogeneous expression of IL-13Rα2, particularly in samples from advanced stages of melanoma. The IL13Rα2-CD3 BTE facilitated T-cell activation and proliferation by bridging melanoma cells and T cells. We also observed the ability of IL13Rα2-CD3 BTE to direct T cells to kill multiple melanoma patient-derived cell lines through xCELLigence assay in vitro, including those with various mutations associated with late-stage metastatic melanoma. IL13Rα2-CD3 dBTE expressed in vivo led to notable tumor regression through inducing increased T-cell infiltration and activation within the tumor microenvironment.

Conclusions These promising findings underscore the potential of targeting IL13Rα2 as a relevant target for the development of biologics including dBTE aimed at treating specific subsets of melanoma.

WHAT IS ALREADY KNOWN ON THIS TOPIC

⇒ Melanoma is an immunogenic cancer that can respond to immune checkpoint inhibitors, yet many patients experience resistance or relapse. Bispecific T-cell engagers (BTEs) have shown promise in hematologic malignancies and, more recently, in uveal melanoma. However, their application in melanoma remains largely unexplored, particularly using targets that are not major histocompatibility complex (MHC)-restricted.

WHAT THIS STUDY ADDS

⇒ This study identifies interleukin-13 receptor subunit alpha-2 (IL13Rα2) as a therapeutically targetable antigen in a subset of melanoma tumors and presents the first preclinical evaluation of an IL13Rα2-CD3 BTE in melanoma. We demonstrate its ability to engage T cells, induce cytotoxicity against IL13Rα2$^+$ melanoma cells, and extend survival in vivo.

HOW THIS STUDY MIGHT AFFECT RESEARCH, PRACTICE OR POLICY

⇒ These findings support IL13Rα2 as a rational immunotherapeutic target and lay the groundwork for further development of non-MHC-restricted BTEs in melanoma. This approach may benefit patients who are resistant to existing immunotherapies and expand the repertoire of targeted immunotherapies in solid tumors.

INTRODUCTION

Melanoma is the most aggressive type of skin cancer, and the incidence rates have been increasing in the past few years.[1] Although advances in targeted therapies (eg, BRAF/MEK inhibitors) and immune checkpoint inhibitors (ICIs) have significantly improved survival in advanced melanoma, many patients experience resistance or immune escape.[2 3] Chemotherapy remains limited by low response rates and toxicity. ICIs can induce durable responses, but only in a subset of patients, often accompanied by immune-related adverse events. Notably, in 2024, the Food and Drug Administration (FDA) approved lifileucel, a tumor-derived TIL (tumor-infiltrating lymphocyte) therapy, for

patients with unresectable or metastatic melanoma who had progressed after programmed cell death protein-1 (PD-1) blockade and, when appropriate, BRAF-targeted therapy.[4 5] This approval not only affirms the immunogenicity of melanoma but also highlights the presence of functional T cells within the tumor microenvironment, which could be effectively redirected by bispecific T-cell engagers (BTEs). Unlike Chimeric antigen receptor (CAR) T-cell therapy, BTEs are off-the-shelf agents with dose flexibility and rapid pharmacokinetics, allowing for better control of cytokine release syndrome (CRS) and other toxicities. Tebentafusp, an HLA-restricted BTE, demonstrated clinical success in uveal melanoma, supporting further development of BTEs for solid tumors.[6 7] However, broader application in melanoma remains underexplored.

BTEs are a therapeutic modality that can recognize T cells through an anti-CD3 arm and simultaneously bind to targeted antigen-positive cancer cells through a second arm. This structure helps form a synapse between T cells and cancer cells, allowing activated T cells to lyse target cells.[8] The applications of BTEs for hematologic malignancies have shown significant antitumor activity, exemplified by the first FDA-approved BTE, blinatumomab, an anti-CD19×anti-CD3 structure for treating B-cell progenitor acute lymphoblastic leukemia.[9] The development of BTEs for solid tumors has also progressed rapidly. In addition to the gp100-targeting tebentafusp, the potential accelerated approval of tarlatamab-dlle for extensive stage small cell lung cancer therapy is encouraging. Tarlatamab-dlle is a BTE targeting DLL3 and achieved 14.3 months of overall survival based on a recent phase II trial.[10] Other studies with BTEs targeting other tumor-associated antigens (TAAs) are ongoing, such as PSMA, EPCAM, and CD33-targeting BTEs.[11 12] However, clinical studies for melanoma treatment with BTEs are currently very limited, with only one targeting tyrosinase-related protein 1 ongoing (NCT04551352).

Interleukin-13 receptor subunit alpha-2 (IL13Rα2) is a high-affinity membrane receptor for interleukin 13 (IL-13).[13] Cancer-associated chronic inflammation is related to the induction of IL-13, which may consequently promote IL13Rα2 expression.[14] The overexpression of IL13Rα2 has been reported in many cancers and may be correlated with tumor metastases and poor prognosis, such as glioblastoma multiforme (GBM),[15] breast cancer,[16] gastric cancer,[17] and colon cancer.[18] Initial studies in our laboratory identified expression of IL13Rα2 in one patient-derived melanoma cell line. To further explore IL13Rα2 expression profile in human melanoma, we conducted detailed analysis using RNA sequencing data from 378 melanoma patient-derived xenograft (PDX) samples (figure 1). We found that IL13Rα2 was expressed in a subset of patients with melanoma, and higher IL13Rα2 expression was associated with more advanced stages. IL13Rα2 expression at the protein level was also observed in melanoma tissue samples and could also be detected on multiple human melanoma lines. These findings indicate IL13Rα2 as a potential therapeutic target for melanoma treatment.

In this study, we used an IL13Rα2-CD3 DNA-encoded BTE (dBTE) to explore its potential in melanoma immunotherapy. The IL13Rα2-CD3 dBTE directed robust killing of melanoma cells with IL13Ra2 expression in vitro. Multiple melanoma cell lines, displaying heterogeneous IL13Rα2expression levels, were tested. These patient-derived melanoma cell lines were obtained with various gene mutations from different disease stages. Furthermore, to evaluate the in vivo efficacy of IL13Rα2-CD3 dBTE, we employed immunodeficient NOD.Cg-Prkdc^{scid} Il2rg^{tm1Wjl}/SzJ (NSG) mice to establish a human melanoma tumor model, which was subsequently treated with IL13Rα2-CD3 dBTE after reconstitution with human peripheral blood mononuclear cells (PBMCs) or T cells. Our work is the first study of melanoma treatment by targeting IL13Rα2 with a T-cell engager, offering a novel therapeutic approach for a distinct subset of patients whose tumors express IL13Rα2.

METHODS

Cell lines

Human melanoma cell lines WM3734, WM3311, WM1366 and WM3540 were acquired from Meenhard Herlyn's lab (The Wistar Institute). The A375 cell line was gifted by Qiang Zhang (The Wistar Institute). 293T cell was purchased from ATCC (ATCC, CRL-3216). All the above cell lines were maintained in Dulbecco's Modified Eagle's Medium (DMEM) supplemented with 10% fetal bovine serum at 37°C in 5% CO_2. OVCAR3 cell line was provided by J. R. Conejo-Garcia (Department of Immunology, Moffitt Cancer Center, Tampa, Florida). OVISE cell line was provided by R. Zhang (MD Anderson Cancer Center). OVCAR3 and OVISE were cultured in Roswell Park Memorial Institute (RPMI) 1640 medium supplemented with 10% fetal bovine serum at 37°C in 5% CO_2. All the cells were checked to be *Mycoplasma* negative and STR analysis identified.

Human PBMCs from healthy donors were provided by the Human Immunology Core of the University of Pennsylvania.

IL13Rα2-CD3 targeting bispecific antibodies

The design of DNA constructs encoding IL13Rα2-CD3 BTE (PB01-forward) was described previously.[19] These IL13Rα2-CD3 targeting bispecific antibodies were produced by transfecting Expi293F cells (Thermo Fisher, A14527) using Expi293 Expression System Kit (Thermo Fisher, A14635). The construct contained a C-terminal 6×His tag to facilitate purification. Supernatants were harvested after 6 days of transfection and clarified by centrifugation followed by filtration through a 0.22 µm filter. His-tagged BTE was purified using Ni-NTA affinity chromatography (Ni-NTA agarose resin, Qiagen) according to the manufacturer's instructions. Briefly, the filtered supernatant was loaded onto an Ni-NTA column

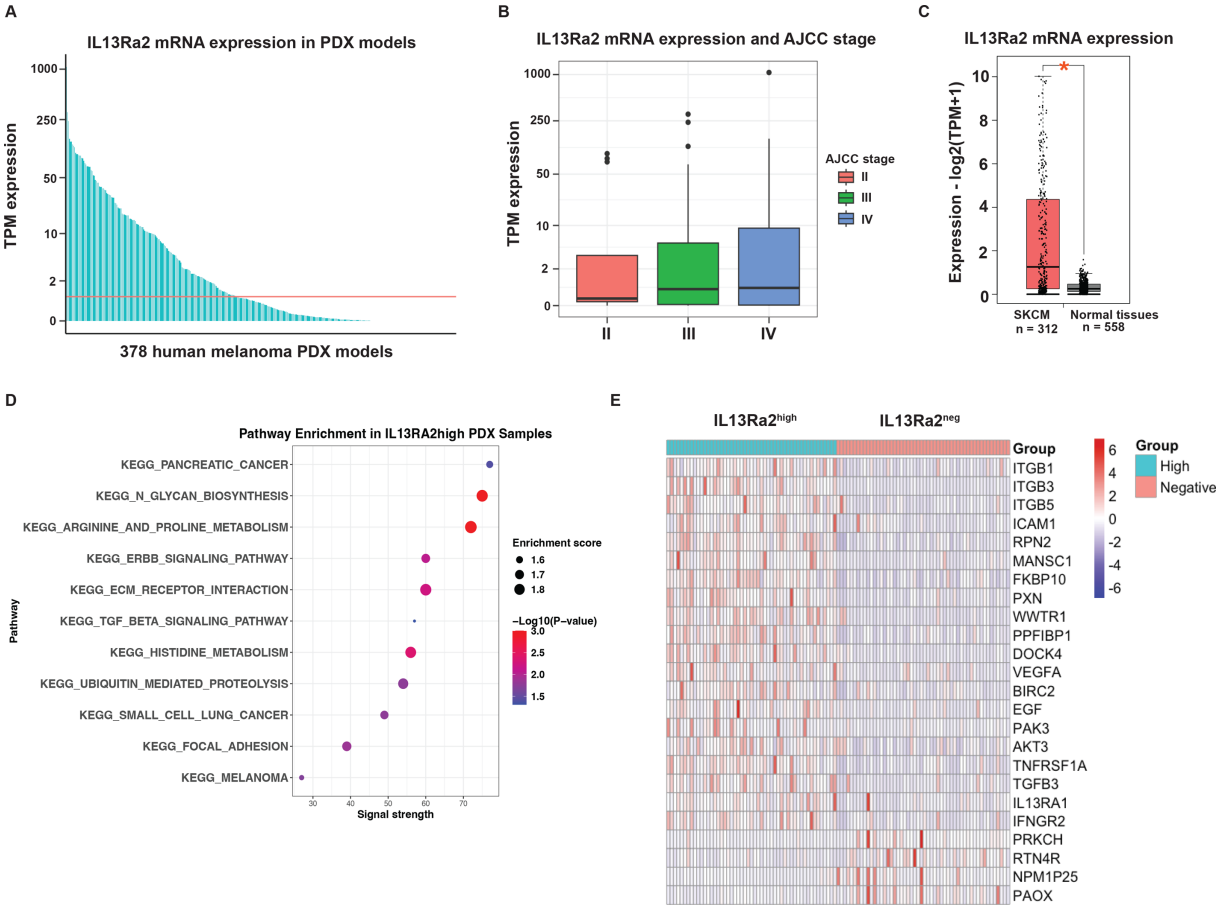

Figure 1 IL13Rα2 is heterogeneously expressed in melanoma PDX models and associated with distinct transcriptomic profiles. This figure characterizes the expression of IL13Rα2 in human melanoma PDX samples and public datasets to support its potential as a therapeutic target. (A) IL13Rα2 mRNA levels across 378 human melanoma PDX samples. (B) Distribution of IL13Rα2 expression by AJCC clinical stage to explore potential stage-related trends. (C) Comparison of IL13Rα2 expression between normal skin and melanoma samples in TCGA using GEPIA2, indicating tumor-specific upregulation. (D) KEGG pathway enrichment analysis of IL13Rα2 ^{high} samples reveals associated biological pathways. (E) Heatmap of differentially expressed genes in IL13Rα2^{high} in comparison to IL13Rα2^{neg} PDX samples, highlighting genes related to immune response and tumor progression. AJCC, American Joint Committee on Cancer; IL13Rα2, interleukin-13 receptor subunit alpha-2; KEGG, Kyoto Encyclopedia of Genes and Genomes; mRNA, messenger RNA; PDX, patient-derived xenograft; TCGA, The Cancer Genome Atlas Program; TPM, transcripts per kilobase million.

equilibrated with binding. After washing with increasing concentrations of imidazole (20–30 mM), the protein was eluted using an elution buffer containing 250 mM imidazole. Eluted fractions were pooled and buffer-exchanged into phosphate-buffered saline using a centrifugal filter unit (Pierce Protein Concentrators PES, 10K MWCO, Thermo). The concentration of protein was quantified by NanoDrop (Thermo).

IL13RA2 mRNA expression in PDX model

Melanoma PDXs were established as previously described.[20–22] Briefly, snap-frozen PDX tumor tissue samples and formalin-fixed paraffin-embedded (FFPE) blocks were sent to Broad Institute and Saint John's Cancer Institute for RNA sequencing (RNA-seq) analyses. The RNA-seq raw data was aligned to the UCSC hg38 reference genome using STAR (V.2.7.11).[23] Gene-level expression quantification was computed using HTSeq (V.2.0.4)[24] and the raw counts were further normalized to TPM (transcripts per kilobase million). Batch effect removal was conducted by ComBat-seq before TPM normalization.[25] For downstream analysis, we stratified the 378 RNA-seq samples based on IL13RA2 TPM values. The PDX samples were then ranked based on IL13RA2 expression levels from highest to lowest. The expression level was correlated with the corresponding clinical data, specifically focusing on the American Joint Committee on Cancer (AJCC) stage. For Gene Set Enrichment Analysis (GSEA), samples with IL13RA2 expression higher than the mean TPM value were categorized as the "High" group, whereas samples with no detectable IL13RA2 expression (TPM value equal to 0) were classified as the "Negative" group. GSEA was then performed to compare the transcriptomic profiles between the High and Negative groups.[26] IL13RA2 expression was also analyzed by using the GEPIA2 platform, which is based on The Cancer Genome Atlas Program (TCGA) and Genotype-Tissue

Expression (GTEx) datasets.[27] IL13RA2 expression in melanoma subtypes with different genetic mutations was also analyzed.

Immunofluorescence and immunohistochemistry assay

Human melanoma tissue samples were purchased from TissueArray.Com LLC (Cat# ME1002b). The unstained formalin-fixed paraffin-embedded tissue specimens were baked for 30 min at 60°C before putting into xylene for de-paraffinization. Then antigen retrieval was performed by immersing the slides into 95°C sodium citrate buffer for 15 min. The slides were blocked and incubated with IL13Rα2-CD3 BTE 5 µg/mL overnight. After washing, the slides were incubated with 5 µg/mL AF647 anti-human Fab antibody (Jackson ImmunoResearch, 109-606-006) for 2 hours followed by washing and Nuclear blue (Thermo Fisher, R37606) staining. For analyzing T cell infiltration in A375 tumors in vivo, tumor samples were collected on 7 days post the second immunization. Tumors were sectioned and stained with human CD3 antibody (Agilent, GA503). The slides were scanned using NanoZoomer S60 Digital slide scanner (C13210-01). The images were analyzed and captured using Proscia's digital pathology platform Concentriq.

Flow cytometry analysis

To evaluate IL13Rα2 expression on different cell lines, cells were harvested, counted and 2×10ˆ5 cells each test were plated in a 96-well round bottom plate. Cells were stained with Fixable Viability Dye eFluor 780 (Thermo Fisher, 65-0865-14) and PE anti-human IL13Rα2 antibody (BioLegend, 360306) or PE Mouse IgG1, κ Isotype Ctrl Antibody (BioLegend, 400114) or human IL-13Ra1 PE-conjugated Antibody (R&D systems, FAB1462P). To detect the binding of IL13Rα2-CD3 bispecific antibodies to melanoma cell lines, antibodies at 5 µg/mL were incubated with the indicated melanoma cells. Then Alexa Fluor 647 AffiniPure goat anti-human IgG, F(ab')$_2$ fragment specific (Jackson ImmunoResearch, 109-605-006) was used as secondary antibody. In the indicated experiment, recombinant human IL-13 protein (R&D systems, 213-ILB) was added before binding with PE anti-human IL13Rα2 antibody or bispecific antibodies. After finishing staining, cells were detected by FACSCelesta.

To analyze T-cell activation in vitro, A375 cells were co-cultured with human T cells. IL13Rα2-CD3 BTE at 5 ng/mL was applied for A375 treatment. T cells were collected at 48 hours and stained with Fixable Viability Dye eFluor 780 (Thermo, 65-0865-14), BV650 anti-human CD3 antibody (BioLegend, 317324), BV510 anti-human CD4 antibody (BioLegend, 317444), Pacific blue anti-human CD8 antibody (BioLegend, 344718), APC anti-human CD69 (BD, 555533) and PE/Cy7 anti-human CD25 (BD, 335789). To explore immune cell infiltration into the tumor, a single cell suspension of the tumor was first blocked with Human TruStain FcX (Fc Receptor Blocking Solution) (BioLegend, 422302), and then incubated with a cocktail solution containing Zombie Aqua fixable viability dye (BioLegend, 423102), BV650 anti-human CD3 antibody, FITC anti-human CD4 antibody (BioLegend, 317408), Pacific blue anti-human CD8 antibody and APC anti-human CD69. Cells were acquired using BD FACSymphony A5 SE.

To detect T-cell proliferation in vitro, T cells were labeled with CFSE (BioLegend, 423801), and then cultured with A375 and IL13Rα2-CD3 BTE for 72 hours. T cells were then stained with Fixable Viability Dye eFluor 780 and BV421 anti-human CD3 antibody (BioLegend, 300434). After finishing staining, cells were detected by FACSCelesta. The data was further analyzed using FlowJo software.

xCELLigence RTCA assay

To analyze the efficacy of IL13Rα2-CD3 BTE in vitro, a cell-impedance-based analyzing method was developed using xCELLigence RTCA eSight (Agilent Technologies). Briefly, target cells were plated in an E-plate (Agilent, 300601010). The effector cells, human PBMCs and IL13Rα2-CD3 bispecific antibodies or irrelevant control bispecific antibody were added after 24 hours. The cell index data and images were recorded every 30 min or 4 hours. The data was finally analyzed using RTCA eSight software.

Animal studies

NOD/LtSscidIL2Rγnull (NSG) mice were inbred at The Wistar Institute under license from the Jackson Laboratory (00557). All animal experiments were performed according to the protocol (201410) approved by the Wistar Institute's Institutional Animal Care and User Committee.

To evaluate the potency of IL13Rα2-CD3 targeting bispecific antibodies in vivo, NSG mice were challenged with 1×10^6 A375 or 451LuMR cells subcutaneously. Human PBMCs and DNA constructs encoding IL13Rα2-CD3 bispecific antibodies were injected at indicated time points. Human PBMCs 10×10^6 per mouse were injected intraperitoneally once. The plasmids 100 µg with 24U hyaluronidase were injected intramuscularly, followed by electroporation with the CELLECTRA device (Inovio). Tumor development was monitored two times a week using a caliper. Tumor volume was calculated as (length×width^2/2. Mice were euthanized after observation of graft-versus-host disease or tumor volume reaching 2,000 mm^3, whichever came first.

To explore tumor infiltration of immune cells, the tumors were harvested and dissociated using the human Tumor Dissociation Kit (Miltenyi Biotec, 130-095-929) following the manufacturer's protocols. The samples were filtered through a 40 µm cell strainer (VWR, 542040), and the single-cell suspension was further stained and analyzed by flow cytometry.

Statistics

All statistical analyses were performed using GraphPad Prism V.10. Unpaired Student's t-test was used to analyze

the statistical significance between two groups in tumor weight and T cells tumor infiltration assay. The error bars represent SEM. The comparison of tumor growth between two groups was done by using two-way analysis of variance analysis followed by multiple comparisons test.

RESULTS

IL13Rα2 is heterogeneously expressed in melanoma PDX models and associated with distinct transcriptomic profiles

To explore the general profile of IL13Rα2 expression in human melanoma, we analyzed IL13Rα2 messenger RNA (mRNA) expression distribution from RNA-seq data of 378 samples collected from human PDX models. As shown in figure 1A, IL13Rα2 was expressed heterogeneously by a subset of the samples. It was found that 16.63% of the samples had a TPM value more than 10 for IL13Rα2 expression in mRNA level (online supplemental figure 1A). We then assessed the expression of IL13Rα2 and examined the distribution of these samples across the stages defined by the AJCC. The dataset comprised the following distribution of samples across AJCC stages: stage I (1), stage II (13), stage III (78), and stage IV (234). Our analysis revealed that higher IL13Rα2 expression was associated with more advanced AJCC stages, indicating a potential role of IL13Rα2 in the progression of melanoma (figure 1B). Using the GEPIA2 platform, which is grounded in the TCGA and GTEx datasets, our analysis revealed a statistically significant increase in the expression of IL13Rα2 in skin cutaneous melanoma as compared with normal tissues (figure 1C). Furthermore, our analysis of IL13Rα2 expression across various genetic mutation subtypes revealed heightened expression levels in patients exhibiting BRAF and NF1 mutations (online supplemental figure 1B). To investigate the molecular pathways associated with high IL13RA2 expression, we performed Kyoto Encyclopedia of Genes and Genomes (KEGG) pathway enrichment analysis based on the transcriptomic data of melanoma PDX samples. Several pathways showed significant enrichment in IL13Rα2 high expression samples, including N-Glycan biosynthesis, arginine and proline metabolism, and pancreatic cancer pathways (figure 1D and online supplemental figure 1C). Notably, metabolic and cancer-related signaling pathways such as ERBB signaling, TGF-β signaling, and ECM-receptor interaction were also upregulated. These findings suggest that IL13Rα2^{high} melanomas may exhibit enhanced tumor-promoting signaling and metabolic reprogramming, potentially contributing to aggressive tumor progression. To further investigate the transcriptional landscape associated with elevated IL13Rα2 expression, we compared gene expression profiles between IL13Rα2 high (IL13Rα2^{high}) and (IL13Rα2^{neg}) PDX samples. A heatmap of selected differentially expressed genes revealed distinct clustering patterns between the two groups. IL13Rα2^{high} samples showed upregulation of genes involved in cell adhesion (eg, ITGB1, ITGB3, ICAM1, CDH1), angiogenesis (VEGFA) and apoptosis resistance (BIRC2) (figure 1E). These data suggest that IL13Rα2^{high} tumors may exhibit a more aggressive and immune-evasive phenotype, potentially driven by enhanced integrin signaling and anti-apoptotic mechanisms.

IL13Rα2 expression in human melanoma samples and targeting by bispecific T-cell engager

To validate the expression of IL13Rα2 at the protein level, we conducted immunofluorescence analysis on fixed patient-derived melanoma tissue arrays. IL13Rα2 was found to be undetectable in normal skin tissue (figure 2A). Within human melanoma tissues, the expression of IL13Rα2 was identified on the surface of melanoma cells. In 45 cases of malignant melanoma from different patients, 9 cases were found to show expression of IL13Rα2 at varying levels. Moreover, we also observed increased expression of IL13Rα2 in some human melanoma cell lines by flow cytometry analysis (figure 2B). The IL13Rα2 detecting antibody was further titrated to test the mean fluorescence intensity, indicating variable IL13Rα2 expression levels on different cell lines (figure 2C). But IL13Rα2 was undetectable in 293T and another two ovarian cancer cell lines OVCAR3 and OVISE (online supplemental figure 2A and figure 2B). The melanoma cell lines included in the study were sourced from different stages and exhibited diverse gene mutations. The comprehensive details of the used cell lines can be found in online supplemental table 1.

To investigate whether we can treat melanoma by targeting IL13Rα2, a BTE IL13Rα2-CD3 BTE (PB01-forward) was constructed by fusing anti-CD3 single-chain variable fragment (ScFv) (clone UCHT1) and anti-IL13Rα2 ScFv (clone hu07) using a GS linker.[19 28] Hence, the IL13Rα2-CD3 BTE has the capability to bring T cells into proximity with tumor cells, concurrently activating T cells through the CD3 signaling pathway (figure 2D). We demonstrated the binding of IL13Rα2-CD3 BTE to the IL13Rα2+melanoma cell line A375 and CD3+T cells using flow cytometry (figure 2E). To investigate whether the bispecifics induce IL13Rα2 internalization on binding, we incubated His-tagged bispecifics with A375 cells for 24 hours. Following incubation, the bispecifics were detected using an anti-His antibody, and IL13Rα2 was detected using a specific IL13Rα2 antibody. The results showed that neither the bispecifics nor IL13Rα2 underwent internalization and remained on the cell surface (online supplemental figure 3A). To explore whether the binding of IL13Rα2-CD3 BTE to IL13Rα2 would be blocked by IL-13, IL-13 was incubated with A375 cells before the binding of IL13Rα2-CD3 BTE (online supplemental figure 3B). A commercially available human IL13Rα2 antibody (clone 47) served as the control and demonstrated binding to A375 cells. However, the binding was significantly inhibited by elevated IL-13 levels, particularly when IL-13 exceeded 50 ng/mL. In contrast, the control cytokine IL-17A did not affect the binding of the IL13Rα2 antibody to A375 cells. IL13Rα2-CD3 BTE

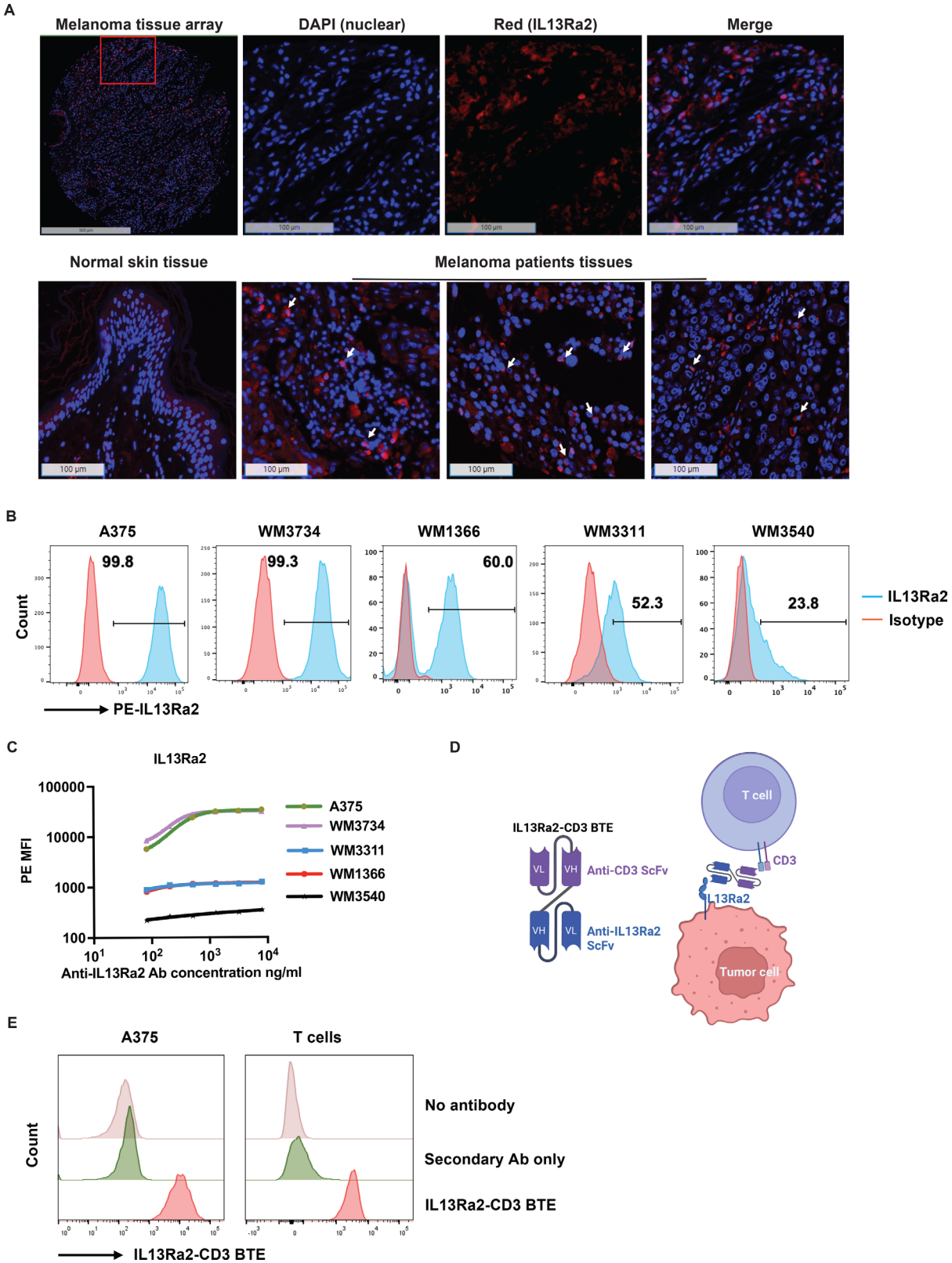

Figure 2 IL13Rα2 expression in human melanoma samples and targeting by bispecific T-cell engager. This figure establishes IL13Rα2 expression in clinical samples and cell lines and confirms binding of the IL13Rα2-CD3 BTE to target and effector cells. (A) Immunofluorescence staining of IL13Rα2 protein in patient-derived melanoma tissue sections. The white arrow indicates the IL13Ra2 expression. (B) Flow cytometric detection of IL13Rα2 surface expression on various melanoma cell lines. (C) Quantification of IL13Rα2 expression by titration of anti-IL13Rα2 antibody and measurement of mean fluorescence intensity (MFI). (D) Schematic illustration of the IL13Rα2-CD3 bispecific T-cell engager design and proposed mechanism of action. (E) Binding analysis of the IL13Rα2-CD3 BTE to both IL13Rα2^{+} A375 melanoma cells and human T cells by flow cytometry. BTE, bispecific T-cell engager; IL13Rα2, interleukin-13 receptor subunit alpha-2; ScFv, single-chain variable fragment.

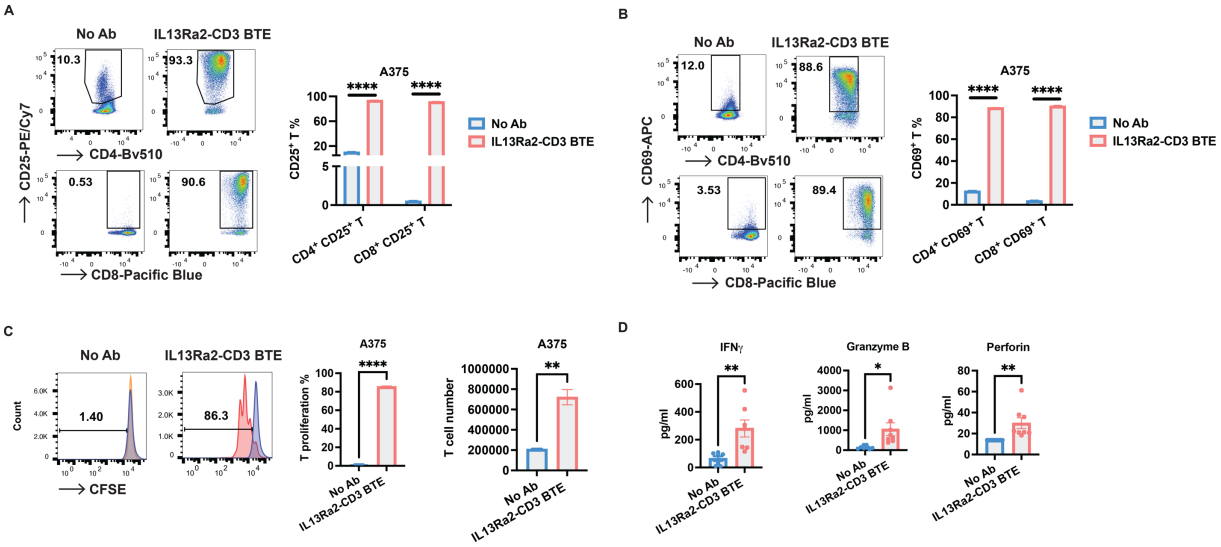

Figure 3 IL13Rα2-CD3 BTE promotes T-cell activation, proliferation, and cytokine secretion in vitro. This figure evaluates the functional activation of T cells following engagement by IL13Rα2-CD3 BTE in co-culture with IL13Rα2-expressing melanoma cells. (A–B) T-cell activation was assessed by flow cytometry following 48-hour co-culture of human T cells with A375 melanoma cells and 5 ng/mL IL13Rα2-CD3 BTE, measuring surface expression of activation markers CD25 and CD69. (C) T-cell proliferation was measured using CFSE-labeled T cells co-cultured with A375 cells and 5 ng/mL IL13Rα2-CD3 BTE for 72 hours. (D) Cytokine secretion was quantified from culture supernatants using a LEGENDplex assay, reflecting immune activation in response to BTE treatment. T cells from one healthy donor were used for the assay, and each condition was tested in three technical replicates. Statistical significance was determined by Student's t-test. *p<0.05, **p<0.01, ****p<0.0001. BTE, bispecific T-cell engager; CFSE, carboxyfluorescein succinimidyl ester; IL13Rα2, interleukin-13 receptor subunit alpha-2.

effectively bound to A375 cells, despite the presence of high levels of IL-13. This finding suggests that IL-13 could not block the binding of IL13Rα2-CD3 BTE to IL13Rα2 expressed by melanoma cells.

We further explored the function of IL13Rα2-CD3 BTE in mediating T-cell activation and proliferation in vitro. A375 cells were co-cultured with T cells in the presence of IL13Rα2-CD3 BTE. T-cell expression of CD25 and CD69 was assessed by flow cytometry. We observed a significant increase in $CD25^+$ and $CD69^+$ T cells with IL13Rα2-CD3 BTE treatment compared with no antibody control (figure 3A,B). T-cell proliferation was tracked by labeling with carboxyfluorescein succinimidyl ester (CFSE). After co-culturing with A375 cells for 72 hours, T cells showed no proliferation in the absence of antibody treatment. However, T cells underwent three divisions when treated with IL13Rα2-CD3 BTE (figure 3C). This treatment significantly increased both the percentage of daughter T cells and the total number of T cells. Additionally, analysis of the cell culture supernatant revealed significantly higher concentrations of interferon-γ, granzyme B, and perforin in the IL13Rα2-CD3 BTE treatment compared with the control with no antibody (figure 3D). In conclusion, these results suggest that IL13Rα2-CD3 BTE induced T-cell activation and proliferation in melanoma treatment.

IL13Rα2-CD3 BTE demonstrated dose-dependent cytotoxicity against human melanoma cells with IL13Rα2 expression in vitro

Next, we tested the tumor-killing effect of IL13Rα2-CD3 BTE for human melanoma treatment in vitro using a cell-impedance-based xCELLigence RTCA. The target cells were plated 24 hours before the addition of human PBMCs and IL13Rα2-CD3 BTE for treatment. The growth of target cells was monitored by recording an increased cell index, while cell apoptosis was reflected in a reduced cell index. We then analyzed the efficacy of IL13Rα2-CD3 BTE in inducing the killing of human melanoma cells with IL13Rα2 expression in vitro. IL13Rα2-CD3 BTE led to the killing of all target cells at 250 ng/mL and 15.63 ng/mL doses (figure 4A–E). However, with a low concentration of IL13Rα2-CD3 BTE treatment at 0.24 ng/mL, we only observed partial killing of A375, WM3734 and WM1366. No difference was observed between No Ab and 0.24 ng/mL treatment for WM3540 and WM3311. Representative images were shown in online supplemental figure 4A. Moreover, we analyzed the cytolysis of target cells compared with the No Ab control. The IL13Rα2-CD3 BTE exhibited dose-dependent cytotoxicity against the target cells, and a decrease in the killing of target cells was observed with a reduction in the titration of IL13Rα2-CD3 BTE (online supplemental figure 4B). The EC50 (half-maximal effective concentration) of IL13Rα2-CD3 BTE was calculated, with EC50 for these cell lines below 5 ng/mL (92.59 pM). The EC50 for A375 (100% IL13Rα2+) was 0.366 ng/mL (6.78 pM). The EC50 of tebentafusp for Mel526 or Mel624 cells were around 50

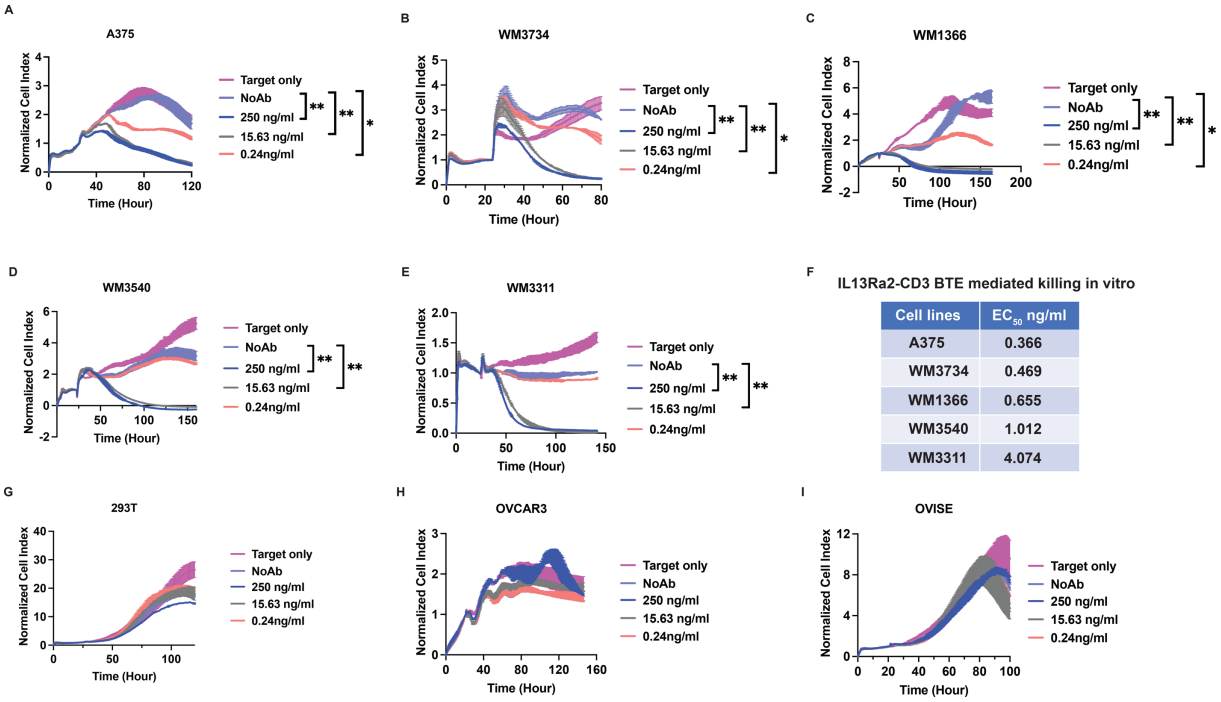

Cell lines	EC_{50} ng/ml
A375	0.366
WM3734	0.469
WM1366	0.655
WM3540	1.012
WM3311	4.074

Figure 4 IL13Rα2-CD3 BTE demonstrated dose-dependent cytotoxicity against human melanoma cells with IL13Rα2 expression in vitro. This figure assesses the cytolytic activity of IL13Rα2-CD3 BTE using a real-time cell analysis platform. (A–F) Cytotoxicity was measured using xCELLigence RTCA assay across multiple IL13Rα2$^+$ human melanoma cell lines. Target cells were seeded 24 hours prior to the addition of human PBMCs and varying concentrations of IL13Rα2-CD3 BTE. Cell index was monitored every 30 min and normalized at the time of treatment, demonstrating dose-dependent killing. (G–I) Control experiments using IL13Rα2$^-$ cell lines (293T, OVCAR3, and OVISE) showed minimal cytotoxic effects, confirming target-specific activity. The cytotoxicity assays were performed at least three times using PBMCs from different healthy donors. Each assay included two technical replicates per condition. Statistical significance was determined by two-way analysis of variance comparing no antibody control and BTE-treated groups. *p<0.05, **p<0.01. BTE, bispecific T-cell engager; EC50, half-maximal effective concentration; IL13Rα2, interleukin-13 receptor subunit alpha-2; PBMCs, peripheral blood mononuclear cells.

pM, which used purified CD8$^+$T for analyses.[29] However, the IL13Rα2-CD3 BTE showed no effect on IL13Ra2-cell lines 293T, OVCAR3 and OVISE (figure 4G–I). To assess whether the presence of IL-13 influences the activity of the bispecifics, we conducted cytotoxicity assays using A375 and WM3734 cells in the presence of varying concentrations of IL-13. The addition of IL-13 had no impact on the bispecific-mediated cytotoxicity against these cells (online supplemental figure 4C). We also evaluated the effect of an irrelevant BTE on A375, WM3311 and WM3540. No killing of the target cells was observed in all these three cell lines with different concentrations of irrelevant BTE treatment, as shown in the cell index curves and representative images (online supplemental figure 4D). In conclusion, these results suggest that IL13Rα2-CD3 BTE could induce the killing of human melanoma cells with IL13Rα2 expression.

IL13Rα2-CD3 dBTE led to human melanoma tumor regression in vivo

To evaluate the potency of IL13Rα2-CD3 BTE in vivo, we established A375 tumor models in immunodeficient NSG mice. A375 tumors were then treated with human PBMCs and DNA-encoded IL13Rα2-CD3 BTE (IL13Rα2-CD3 dBTE) by using electroporation (EP) injection of a plasmid encoding IL13Rα2-CD3 BTE. Initially, a single dosage of 100 µg IL13Rα2-CD3 dBTE was injected 5 days post A375 inoculation (figure 5A), with EP injection of water and human PBMCs transfer as a mock control. However, no significant tumor inhibition was observed through monitoring tumor development. Compared with the mock control, tumor growth only showed a mild growth delay with IL13Rα2-CD3 dBTE treatment (figure 5B). Considering the rapid clearance of BTE in vivo,[30] mice were injected with IL13Rα2-CD3 dBTE weekly for three consecutive weeks (figure 5C). We used either human PBMCs or T cells as effector cells, with the injection of 10 million cells per mouse. A375 tumors without treatment grew rapidly, and all mice reached the endpoint (tumors around 2,000 mm^3) before 40 days. Compared with the mock groups, A375 tumor development was significantly inhibited with IL13Rα2-CD3 dBTE multiple doses of treatment, using either PBMCs (figure 5D) or T cells (online supplemental figure 5A) as effector cells. In the IL13Rα2-CD3 dBTE treatment with PBMCs, tumors were eliminated in two out of five mice. However, tumors that did not disappear exhibited slow and continued growth (online supplemental figure 5B). Moreover, IL13Rα2-CD3 dBTE treatment significantly prolonged the survival of mice compared with the mock-treated group, prior to euthanasia due to severe graft-versus-host disease

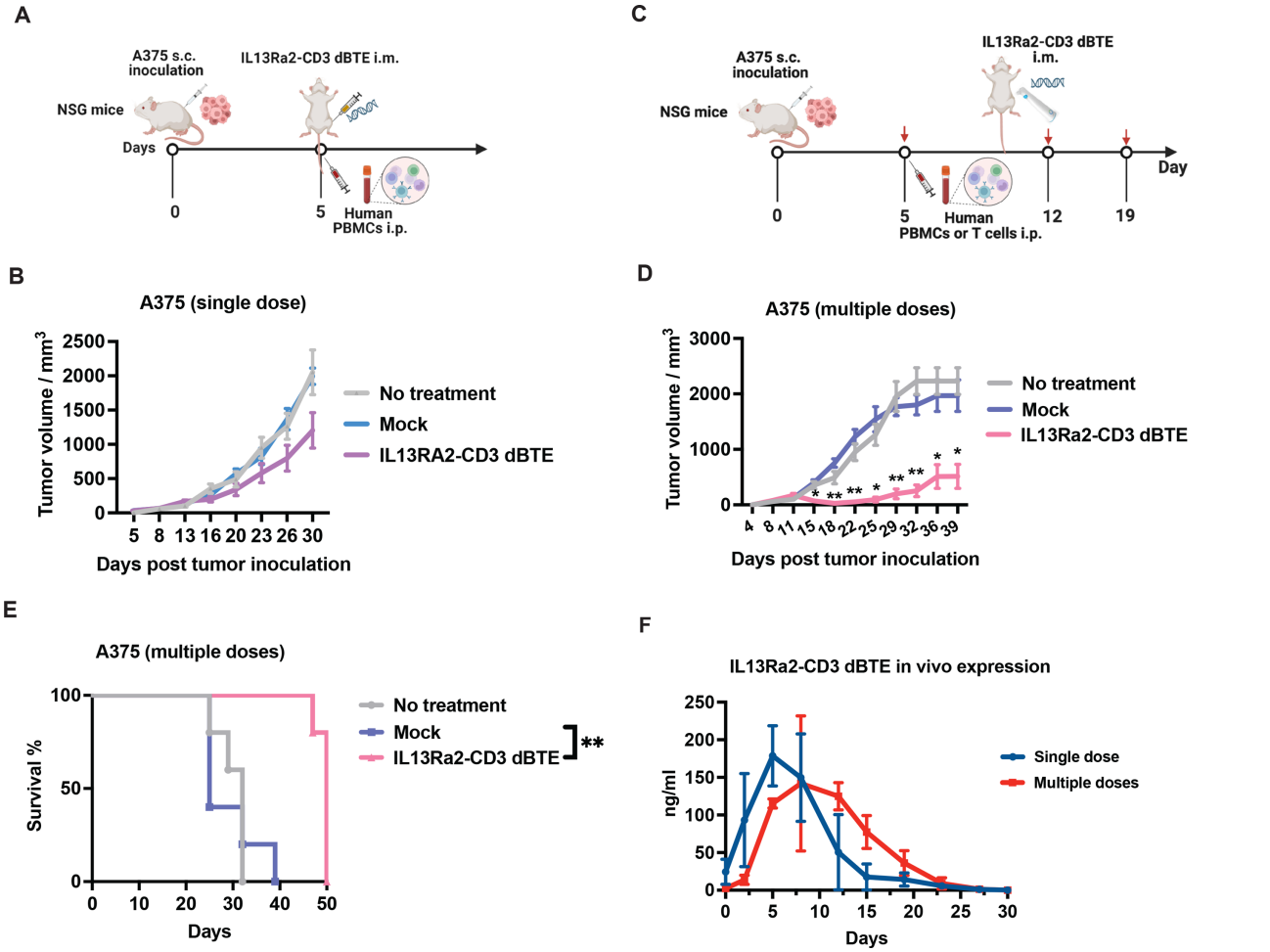

Figure 5 IL13Rα2-CD3 dBTE led to A375 melanoma tumors regression in vivo. This figure evaluates the antitumor efficacy of DNA-encoded IL13Rα2-CD3 bispecific T-cell engager (dBTE) in vivo. (A) Schematic overview of the experimental design for single-dose treatment. NSG mice were subcutaneously implanted with A375 melanoma cells, and 10×10⁶ human PBMCs were administered intraperitoneally on day 5. A single intramuscular injection of 100 µg IL13Rα2-CD3 dBTE was delivered on the same day, followed by electroporation (n=5). (B) Tumor growth curves following single-dose dBTE treatment. (C) Schematic of the multiple-dose treatment strategy involving weekly administration of IL13Rα2-CD3 dBTE for a total of three doses, in combination with either human PBMCs or purified T cells. (D) Tumor growth curves for the multiple-dose regimen using PBMCs. (E) Kaplan-Meier survival analysis of treated mice. (F) In vivo expression levels of IL13Rα2-CD3 dBTE after single or repeated dosing. Tumor growth was analyzed by two-way analysis of variance with multiple comparisons; survival data were analyzed using the log-rank (Mantel-Cox) test. *p<0.05, **p<0.01. IL13Rα2, interleukin-13 receptor subunit alpha-2; i.m., intramuscular; i.p., intraperitoneally; PBMCs, peripheral blood mononuclear cells; s.c., subcutaneously.

(figure 5E). To evaluate the pharmacokinetic profile of IL13Rα2-CD3 dBTE expression in vivo, we tested the bispecifics level in serum following either a single dose or multiple dosing regimen. As shown in figure 5F, peak expression was observed around day 5 in the single dose regimen, followed by a rapid decline. In contrast, multiple dosing maintained elevated the bispecific levels over a longer period, with more sustained expression beyond day 15. These data suggest that repeated dBTE administration enhances the duration of systemic availability. In conclusion, these results suggest that IL13Rα2-CD3 dBTE is effective in vivo in inhibiting melanoma tumor development through multiple injections.

IL13Rα2-CD3 dBTE promoted T cells infiltration and activation in the tumor microenvironment

To further characterize IL13Rα2-CD3 dBTE activity in vivo, we collected A375 tumor samples after two doses of IL13Rα2-CD3 dBTE treatment and analyzed T cells infiltration in the tumors by flow cytometry (figure 6A). Through measuring tumor weight, we found that the tumors from the IL13Rα2-CD3 dBTE treatment group were significantly smaller compared with the mock control group (figure 6B). The gating strategy of flow analysis was shown in online supplemental figure 6A. We found increased $CD3^+$ T cells, $CD4^+$ T cells and $CD8^+$ T cells infiltration in the tumor microenvironment after IL13Rα2-CD3 dBTE treatment (figure 6C–E). We also observed a trend toward increased $CD4^+CD69^+$ T cells but not reaching statistical significance (figure 6F). However,

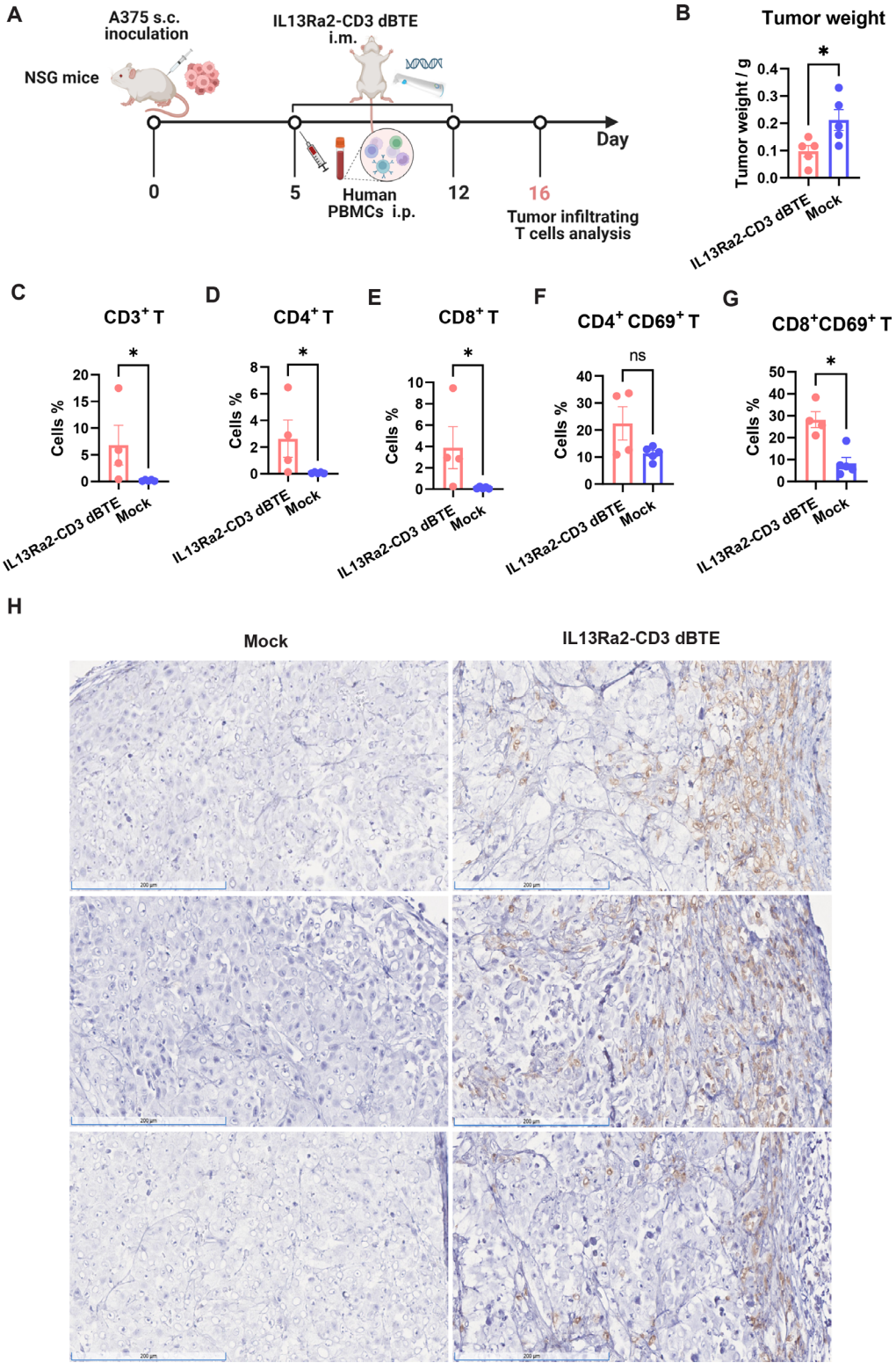

Figure 6 IL13Rα2-CD3 dBTE promoted T cell infiltration and activation in the tumor microenvironment. This figure investigates the impact of IL13Rα2-CD3 dBTE on T-cell infiltration into A375 melanoma tumors in vivo. (A) Schematic of the experimental timeline: NSG mice were subcutaneously implanted with A375 melanoma cells and received 10×10^6 human PBMCs intraperitoneally on day 5. IL13Rα2-CD3 dBTE was administered intramuscularly on days 5 and 12 (n=5). (B) Tumor weights were measured at endpoint. (C–G) Flow cytometry analysis of tumor-dissociated cells revealed the percentages of infiltrating human T cells and T cells. $CD3^+$ T cells were gated from live cells; $CD4^+$ and $CD8^+$ subsets were further gated from $CD3^+$ T cells. $CD69^+$ cells were quantified within each subset. (H) Immunohistochemistry analysis of $CD3^+$ T-cell distribution in tumor sections confirmed enhanced infiltration. Statistical significance was assessed using Student's t-test. *p<0.05. dBTE, DNA encoded bispecific T-cell engager; IL13Rα2, interleukin-13 receptor subunit alpha-2; i.m., intramuscular; i.p., intraperitoneally; PBMCs, peripheral blood mononuclear cells; s.c., subcutaneously.

$CD8^+CD69^+$ T cells were significantly increased with IL13Rα2-CD3 dBTE treatment (figure 6G). Through immunohistochemical analysis of tumor sections, a marked increase of CD3+T cells infiltration was observed in the IL13Rα2-CD3 dBTE treatment group compared with the mock controls. Tumors from dBTE-treated mice exhibited prominent T-cell presence, particularly at the tumor margins and stromal regions, while mock-treated tumors showed minimal T-cell infiltration (figure 6H). These findings suggest that IL13Rα2-CD3 dBTE effectively promotes T-cell recruitment to the tumor microenvironment.

DISCUSSION

In this study, we investigated IL13Rα2 expression in melanoma by employing RNA-seq analysis of melanoma PDX models and analyzing the TCGA database based on samples from patients with cutaneous melanoma. PDX models serve as a living tumor bank established in immunodeficient NSG mice, using primary tissues derived from patients across various melanoma stages and subtypes. This includes samples from therapy-naïve individuals as well as those who have acquired resistance to therapy.[20 22] Therefore, PDX models are accurate resources to analyze TAA expression in clinical settings. There are some indications that IL13Rα2 is overexpressed in a subset of melanomas.[31 32] But this is the first study exploring IL13Ra2 expression using melanoma PDX models. In our analysis with PDX models, we found that IL13Rα2 was expressed heterogeneously in 378 samples, with IL13Rα2 expression distributed in late stages (III and IV) of melanoma. In the TCGA database, IL13Rα2 was also found to have increased expression in cutaneous melanoma, particularly in patients with BRAF and NF1 mutations. According to a TCGA program study on cutaneous melanoma, there were around 52% of patients with BRAF mutations, 28% with RAS mutations and 14% with NF1 mutations.[33] Studies also reported that the BRAF mutations were not only associated with melanogenesis but also could promote tumor metastasis.[34 35] Thus, high expression of IL13Rα2 in melanoma with BRAF mutations may indicate its accumulated expression in late-stage melanoma. In conclusion, these findings suggest IL13Rα2 as a promising target for melanoma treatment, especially for patients in advanced stages with resistance to targeted therapies.

The advancements in melanoma treatments, encompassing targeted therapies and immunotherapies, have illuminated new possibilities in the approach to treating this condition. Nevertheless, their application and impact remain constrained. The acquired resistance to targeted therapies poses a significant challenge.[36] The responses of patients to immunotherapies are also influenced by many factors, such as tumor immune status or immune evasion.[37] Hence, ongoing research for innovative immunotherapies, particularly tailored for late-stage melanoma treatment, remains imperative. Previous studies of immune cell engagers targeting IL13Rα2 have focused on GBM.[38 39] In our recent study, we designed IL13Rα2 targeting BTEs (IL13Rα2-CD3 BTEs) in four different ScFv heavy-light chain orientations.[19] After comparing their efficacy and specificity, we selected one orientation for an in vivo GBM challenge study using dBTE (IL13Rα2-CD3 dBTE). IL13Rα2-CD3 dBTE induced significant antitumor activity and controlled tumor development in an orthotopic GBM model. In this study, we explored IL13Rα2-CD3 BTE for melanoma immunotherapeutic treatment. Patient-derived melanoma cell lines from different stages with various mutations were collected for in vitro studies. We investigated the efficacy of IL13Rα2-CD3 BTE in these melanoma cell lines with IL13Rα2 expression through in vitro killing assay by adding human PBMCs. We found that IL13Rα2-CD3 BTE could induce dose-dependent killing of target cells. This finding suggests that the IL13Rα2-CD3 BTE holds promise for targeted treatment in patients with IL13Rα2+melanoma in the future, with the potential for dose escalation studies.

To the best of our knowledge, only one clinical trial has been disclosed for melanoma treatment involving the targeting of IL13Rα2 through CAR T-cell therapy (NCT04119024). However, BTEs appear to offer greater feasibility in terms of dose manipulation compared with CAR T-cell therapy. BTEs serve as an off-the-shelf alternative to CAR T-cell therapy, and both modalities carry the risk of inducing CRS due to non-specific T-cell activation. Consequently, meticulous dose studies and control become crucial in minimizing the potential side effects of CRS.[40–42] In this study, the application of IL13Rα2-CD3 BTE for the treatment of melanoma cells with partial IL13Rα2 expression (WM1366 and WM3540) in vitro revealed that BTEs resulted in 100% of target cell killing. This phenomenon may be implicated in the killing of bystander TAA-negative cells. As per a study involving EGFR-targeting BTE, activated T cells demonstrated the capability to kill TAA-negative cells through the ICAM-1 and FAS pathway, particularly when the negative cells were in close proximity to positive cells.[43] But for the in vivo challenge model of A375, with 100% IL13Rα2 expression, the efficacy in eliminating solid tumors became evident, particularly with multiple repeated treatments. While our in vitro studies confirmed the specificity and efficacy of the IL13Rα2-targeted dBTE, subsequent in vivo testing in two PDX melanoma models did not demonstrate significant tumor suppression. One notable feature was the slow and delayed tumor development, which may have contributed to adaptive antigen loss or downregulation over time. Interestingly, tumors from the treated groups appeared more rounded in morphology, and immunohistochemical analysis revealed that $CD3^+$ T cells were largely confined to the tumor periphery, with minimal infiltration into the tumor core. This pattern suggests immune exclusion, a known resistance mechanism in solid tumors, where T cells are physically or functionally blocked from accessing the tumor interior despite being

recruited. These findings indicate that T-cell engagement did occur but was likely insufficient for effective tumor clearance due to poor infiltration or limited antigen availability. Moving forward, we aim to improve dBTE efficacy by incorporating multivalent targeting of additional melanoma-associated antigens, extending the half-life and exploring strategies to overcome immune exclusion, such as combining with agents that modulate the tumor microenvironment.

Acknowledgements We are grateful to The Wistar Institute's Animal Facility, Histotechnology Facility, Imaging Facility, Flow Cytometry Facility, Biomedical Research Support Facility and Research Supply Center for providing technical support. We thank biostatistician Qin Liu at The Wistar Institute for providing consultation about statistical analysis. We thank Min Xiao and Qiang Zhang at The Wistar Institute for providing the melanoma cell lines. We thank Emily Cento, Zhilin Chen, Max A Eldabbas, and Emileigh Maddox of the Human Immunology Core and the Division of Transfusion Medicine and Therapeutic Pathology at the Perelman School of Medicine at the University of Pennsylvania for providing de-identified, human PBMCs and T cells that were purified from healthy donor apheresis using StemCell RosetteSep kits. The HIC is supported in part by NIH P30 AI045008 and P30 CA016520. HIC RRID: SCR_022380. The experimental illustration figures were created by using BioRender (Biorender.com).

Contributors SZ, MH and DBW conceptualized the study and designed the experiments. SZ, PSB and DHP designed the structures of antibodies. SZ and YC acquired and analyzed the data. SZ, PSB, CL, JJ and YG performed experiments. SZ and DBW reviewed the figures and contents. SZ, YC and DBW wrote the manuscript. All authors contributed to the writing and revision of the manuscript. SZ and DBW act as the guarantors for this manuscript.

Funding This work was supported by Wistar/UPenn SPORE in Skin Cancer (NIH - P50 CA261608), the WW Smith Charitable Trust and the Fishman Foundation. This study received funding in part by Inovio Pharmaceuticals. Funding support for The Wistar Institute core facilities was provided by Cancer Center Support Grant P30 CA010815. This work is supported by NIH grants P01 CA114046, U54 CA224070, SPORE P50 CA174523, and the Dr. Miriam and Sheldon G. Adelson Medical Research Foundation.

Competing interests DBW has received grant funding, participates in industry collaborations, has received speaking honoraria, and has received fees for consulting, including serving on scientific review committees. Remunerations received by DBW include direct payments and equity/options. DBW also discloses the following associations with commercial partners: Geneos (consultant/advisory board), AstraZeneca (advisory board, speaker), Inovio (board of directors, consultant), Sanofi (advisory board), Pfizer (advisory board), and Advaccine (consultant). The other authors declare that they have no competing interests.

Patient consent for publication Not applicable.

Ethics approval Not applicable.

Provenance and peer review Not commissioned; externally peer reviewed.

Data availability statement Data are available upon reasonable request. All data relevant to the study are included in the article or uploaded as supplementary information. RNA sequencing data from the melanoma PDX models used for IL13RA2 expression profiling are not publicly available but may be shared upon reasonable request. Correlative analyses of other immune-related genes will be published in a separate manuscript currently in preparation. All other data supporting the findings of this study are available within the article and its supplementary files or from the corresponding author upon request.

Author note DBW is the Executive Vice President and Director of the Vaccine & Immunotherapy Center at The Wistar Institute. He is the WW Smith Distinguished Chair in Cancer Research and Professor Emeritus at University of Pennsylvania Perelman School of Medicine.

ORCID iDs
Shushu Zhao http://orcid.org/0000-0001-5265-9681
Pratik S Bhojnagarwala http://orcid.org/0000-0002-9403-5276
Joshua Jose http://orcid.org/0009-0007-3123-7536
Daniel H Park http://orcid.org/0000-0002-2773-320X
David B Weiner http://orcid.org/0000-0002-2232-8512

REFERENCES

1 Lapides R, Saravi B, Mueller A, *et al*. Possible Explanations for Rising Melanoma Rates Despite Increased Sunscreen Use over the Past Several Decades. *Cancers (Basel)* 2023;15:5868.
2 Patel M, Eckburg A, Gantiwala S, *et al*. Resistance to Molecularly Targeted Therapies in Melanoma. *Cancers (Basel)* 2021;13:1115.
3 Ziogas DC, Theocharopoulos C, Koutouratsas T, *et al*. Mechanisms of resistance to immune checkpoint inhibitors in melanoma: What we have to overcome? *Cancer Treat Rev* 2023;113:102499.
4 Smithy JW, Schoenfeld AJ, Betof Warner A. The Clinical TIL Experience in Melanoma: Past, Present, Future. *Transplant Cell Ther* 2025;31:S626–34.
5 Sarnaik AA, Hamid O, Khushalani NI, *et al*. Lifileucel, a Tumor-Infiltrating Lymphocyte Therapy, in Metastatic Melanoma. *J Clin Oncol* 2021;39:2656–66.
6 Chen LN, Carvajal RD. Tebentafusp for the treatment of HLA-A*02:01-positive adult patients with unresectable or metastatic uveal melanoma. *Expert Rev Anticancer Ther* 2022;22:1017–27.
7 Hassel JC, Piperno-Neumann S, Rutkowski P, *et al*. Three-Year Overall Survival with Tebentafusp in Metastatic Uveal Melanoma. *N Engl J Med* 2023;389:2256–66.
8 Baeuerle PA, Wesche H. T-cell-engaging antibodies for the treatment of solid tumors: challenges and opportunities. *Curr Opin Oncol* 2022;34:552–8.
9 Tian Z, Liu M, Zhang Y, *et al*. Bispecific T cell engagers: an emerging therapy for management of hematologic malignancies. *J Hematol Oncol* 2021;14:75.
10 Ahn M-J, Cho BC, Felip E, *et al*. Tarlatamab for Patients with Previously Treated Small-Cell Lung Cancer. *N Engl J Med* 2023;389:2063–75.
11 Shanshal M, Caimi PF, Adjei AA, *et al*. T-Cell Engagers in Solid Cancers-Current Landscape and Future Directions. *Cancers (Basel)* 2023;15:2824.
12 Arvedson T, Bailis JM, Britten CD, *et al*. Targeting Solid Tumors with Bispecific T Cell Engager Immune Therapy. *Annu Rev Cancer Biol* 2022;6:17–34.
13 Knudson KM, Hwang S, McCann MS, *et al*. Recent Advances in IL-13Rα2-Directed Cancer Immunotherapy. *Front Immunol* 2022;13:878365.
14 Jaén M, Martín-Regalado Á, Bartolomé RA, *et al*. Interleukin 13 receptor alpha 2 (IL13Rα2): Expression, signaling pathways and therapeutic applications in cancer. *Biochim Biophys Acta Rev Cancer* 2022;1877:188802.
15 Zeng J, Zhang J, Yang Y-Z, *et al*. IL13RA2 is overexpressed in malignant gliomas and related to clinical outcome of patients. *Am J Transl Res* 2020;12:4702–14.
16 Márquez-Ortiz RA, Contreras-Zárate MJ, Tesic V, *et al*. IL13Rα2 Promotes Proliferation and Outgrowth of Breast Cancer Brain Metastases. *Clin Cancer Res* 2021;27:6209–21.
17 Lin C, Liu H, Zhang H, *et al*. Interleukin-13 receptor α2 is associated with poor prognosis in patients with gastric cancer after gastrectomy. *Oncotarget* 2016;7:49281–8.
18 Barderas R, Bartolomé RA, Fernandez-Aceñero MJ, *et al*. High expression of IL-13 receptor α2 in colorectal cancer is associated with invasion, liver metastasis, and poor prognosis. *Cancer Res* 2012;72:2780–90.
19 Bhojnagarwala PS, O'Connell RP, Park D, *et al*. *In vivo* DNA-launched bispecific T cell engager targeting IL-13Rα2 controls tumor growth in an animal model of glioblastoma multiforme. *Mol Ther Oncolytics* 2022;26:289–301.

20 Krepler C, Sproesser K, Brafford P, *et al*. A Comprehensive Patient-Derived Xenograft Collection Representing the Heterogeneity of Melanoma. *Cell Rep* 2017;21:1953–67.
21 Garman B, Anastopoulos IN, Krepler C, *et al*. Genetic and Genomic Characterization of 462 Melanoma Patient-Derived Xenografts, Tumor Biopsies, and Cell Lines. *Cell Rep* 2017;21:1936–52.
22 Xiao M, Rebecca VW, Herlyn M. A Melanoma Patient-Derived Xenograft Model. *J Vis Exp* 2019;2019:147.
23 Dobin A, Davis CA, Schlesinger F, *et al*. STAR: ultrafast universal RNA-seq aligner. *Bioinformatics* 2013;29:15–21.
24 Anders S, Pyl PT, Huber W. HTSeq--a Python framework to work with high-throughput sequencing data. *Bioinformatics* 2015;31:166–9.
25 Zhang Y, Parmigiani G, Johnson WE. *ComBat-seq*: batch effect adjustment for RNA-seq count data. *NAR Genom Bioinform* 2020;2:lqaa078.
26 Subramanian A, Tamayo P, Mootha VK, *et al*. Gene set enrichment analysis: a knowledge-based approach for interpreting genome-wide expression profiles. *Proc Natl Acad Sci U S A* 2005;102:15545–50.
27 Tang Z, Kang B, Li C, *et al*. GEPIA2: an enhanced web server for large-scale expression profiling and interactive analysis. *Nucleic Acids Res* 2019;47:W556–60.
28 Yin Y, Boesteanu AC, Binder ZA, *et al*. Checkpoint Blockade Reverses Anergy in IL-13Rα2 Humanized scFv-Based CAR T Cells to Treat Murine and Canine Gliomas. *Mol Ther Oncolytics* 2018;11:20–38.
29 Liddy N, Bossi G, Adams KJ, *et al*. Monoclonal TCR-redirected tumor cell killing. *Nat Med* 2012;18:980–7.
30 Schaller TH, Foster MW, Thompson JW, *et al*. Pharmacokinetic Analysis of a Novel Human EGFRvIII:CD3 Bispecific Antibody in Plasma and Whole Blood Using a High-Resolution Targeted Mass Spectrometry Approach. *J Proteome Res* 2019;18:3032–41.
31 Okamoto H, Yoshimatsu Y, Tomizawa T, *et al*. Interleukin-13 receptor α2 is a novel marker and potential therapeutic target for human melanoma. *Sci Rep* 2019;9:1281.
32 Beard RE, Abate-Daga D, Rosati SF, *et al*. Gene expression profiling using nanostring digital RNA counting to identify potential target antigens for melanoma immunotherapy. *Clin Cancer Res* 2013;19:4941–50.
33 Cancer Genome Atlas Network. Genomic Classification of Cutaneous Melanoma. *Cell* 2015;161:1681–96.
34 Alqathama A. BRAF in malignant melanoma progression and metastasis: potentials and challenges. *Am J Cancer Res* 2020;10:1103–14.
35 Castellani G, Buccarelli M, Arasi MB, *et al*. BRAF Mutations in Melanoma: Biological Aspects, Therapeutic Implications, and Circulating Biomarkers. *Cancers (Basel)* 2023;15:4026.
36 Wagstaff W, Mwamba RN, Grullon K, *et al*. Melanoma: Molecular genetics, metastasis, targeted therapies, immunotherapies, and therapeutic resistance. *Genes Dis* 2022;9:1608–23.
37 Thornton J, Chhabra G, Singh CK, *et al*. Mechanisms of Immunotherapy Resistance in Cutaneous Melanoma: Recognizing a Shapeshifter. *Front Oncol* 2022;12:880876.
38 Pawlowski KD, Duffy JT, Tiwari A, *et al*. Bi-Specific Killer Cell Engager Enhances NK Cell Activity against Interleukin-13 Receptor Alpha-2 Positive Gliomas. *Cells* 2023;12:1716.
39 Yin Y, Rodriguez JL, Li N, *et al*. Locally secreted BiTEs complement CAR T cells by enhancing killing of antigen heterogeneous solid tumors. *Mol Ther* 2022;30:2537–53.
40 Markouli M, Ullah F, Unlu S, *et al*. Toxicity Profile of Chimeric Antigen Receptor T-Cell and Bispecific Antibody Therapies in Multiple Myeloma: Pathogenesis, Prevention and Management. *Curr Oncol* 2023;30:6330–52.
41 Frigault M, Rotte A, Ansari A, *et al*. Dose fractionation of CAR-T cells. A systematic review of clinical outcomes. *J Exp Clin Cancer Res* 2023;42:11.
42 Dasyam N, George P, Weinkove R. Chimeric antigen receptor T-cell therapies: Optimising the dose. *Br J Clin Pharmacol* 2020;86:1678–89.
43 Ross SL, Sherman M, McElroy PL, *et al*. Bispecific T cell engager (BiTE®) antibody constructs can mediate bystander tumor cell killing. *PLoS One* 2017;12:e0183390.